

MEASURING AND ALIGNING ABSTRACTION IN VISION-LANGUAGE MODELS WITH MEDICAL TAXONOMIES

Ben Schaper^{1,‡}, Maxime Di Folco^{1,2,3‡}, Bernhard Kainz^{6,7}, Julia A. Schnabel^{1,2,4,5,*}, Cosmin I. Bercea^{1,4,*}

¹ School of Computation, Information and Technology, Technical University of Munich, Germany

² Institute of Machine Learning in Biomedical Imaging, Helmholtz Munich, Germany

³ LTCI, Télécom Paris, Institut Polytechnique de Paris, France ⁴ Munich Center for Machine Learning (MCML)

⁵ School of Biomedical Engineering and Imaging Sciences, King's College London, UK

⁶ Department of Artificial Intelligence in Biomedical Imaging, FAU Erlangen-Nuremberg, Germany

⁷ Department of Computing, Imperial College London, UK

ABSTRACT

Vision-Language Models (VLMs) show strong zero-shot performance for chest X-ray classification, but standard flat metrics fail to distinguish between clinically minor and severe errors. This work investigates how to quantify and mitigate abstraction errors by leveraging medical taxonomies. We benchmark several state-of-the-art VLMs using hierarchical metrics and introduce *Catastrophic Abstraction Errors* to capture cross-branch mistakes. Our results reveal substantial misalignment of VLMs with clinical taxonomies despite high flat performance. To address this, we propose risk-constrained thresholding and taxonomy-aware fine-tuning with radial embeddings, which reduce severe abstraction errors to below 2% while maintaining competitive performance. These findings highlight the importance of hierarchical evaluation and representation-level alignment for safer and more clinically meaningful deployment of VLMs.

Index Terms— Vision-Language Models, CXR, Hierarchical Metrics, Zero-Shot Classification

1. INTRODUCTION

Vision-Language Models (VLMs) have rapidly advanced in recent years, driven by large-scale datasets and architectures capable of aligning images and text in a shared representation space [1, 2]. A key strength of these models is their ability to perform zero-shot classification, where images can be categorised using textual descriptions of diseases or findings without task-specific training.

In the medical domain, publicly available chest X-ray (CXR) datasets such as MIMIC-CXR [3], and PadChest [4] have enabled the adaptation of VLMs to radiology [5, 6, 7]. However, most current evaluations rely on standard metrics such as accuracy or F1-score, which treat all errors equally.

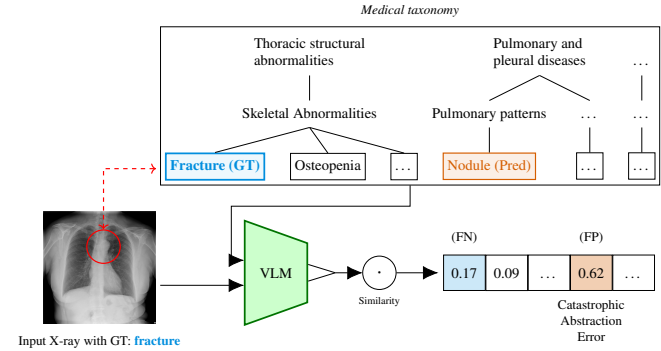


Fig. 1: Illustration of a Catastrophic Abstraction Error (CAE). A chest X-ray with ground truth label *fracture* (FN, blue) is misclassified as *nodule* (FP, orange). Since the prediction and ground truth lie in disjoint branches of the medical taxonomy (top), this cross-branch error constitutes a CAE.

This uniform treatment obscures clinically critical mistakes: a misclassification between closely related findings (e.g., “cardiomegaly” vs. “enlarged cardiac silhouette”) is far less harmful than confusing findings from different categories (e.g., “rib fracture” vs. “pleural effusion”). Flat metrics, therefore, fail to reflect the clinical significance of errors.

Medical taxonomies such as ICD-10 [8] and RadLex [9] provide hierarchical structures that can capture semantic relationships between findings. Integrating these structures into evaluation frameworks allows for a more clinically meaningful assessment of VLMs by distinguishing between minor and catastrophic abstraction errors.

This work investigates how to quantify and mitigate abstraction errors of VLMs in multi-label chest X-ray classification using hierarchical metrics and taxonomy-aware methods. The contributions of this paper are in threefolds: we (i) show that state-of-the-art VLMs remain misaligned with medical taxonomies under hierarchical metrics, (ii) we intro-

‡ Shared first authors

* Co-senior authors

duce a new hierarchical metric tailored to the multi-label setting to capture abstraction errors, and (iii) propose lightweight mitigation strategies, including a risk-constrained strategies for zero-shot multi-label classification and a taxonomy-aware fine-tuning, to reduce severe abstraction errors without compromising standard performance.

2. METHODS

2.1. Benchmarking Setup

To test whether state-of-the-art (SOTA) VLMs are aligned with medical taxonomies, we benchmark their zero-shot performance in a multi-label setting using both flat and hierarchical metrics on PadChest [4]. Here, flat metrics refer to classical evaluation measures that ignore the hierarchical structure, whereas hierarchical metrics explicitly account for it.

Taxonomy Definition: The PadChest-GR dataset contains 4,555 frontal chest X-rays with bilingual, sentence-level annotations, including bounding boxes for localisable findings. These annotations are organised hierarchically, with labels grouped into clinically relevant categories that we adopt as a taxonomy. For this study, we extend the original taxonomy by introducing abstract 3 parent categories showed in Fig. 1, yielding a structured hierarchy of 117 nodes that capture both anatomical and pathological relationships between findings. The complete taxonomy is provided on GitHub¹.

Models: We benchmark a diverse set of SOTA VLMs from both general- and medical-domains: CLIP [1], PubMed-CLIP [6], BiomedCLIP [7], MedCLIP [5], and MedSigLIP².

Metrics: For evaluation, we consider one flat baseline metric and three hierarchical metrics. The flat metric, macro-averaged F_1 -score, serves as a standard, hierarchy-agnostic baseline. To capture clinically meaningful errors, we employ two established hierarchical metrics. The **Hierarchical Overlap Score (HOS)** [10] expands the true and predicted label sets to include all ancestor nodes in the taxonomy. For example, a prediction of “*Fracture*” is augmented with its parent “*Skeletal abnormalities*” and grandparent “*Thoracic structural abnormalities*.” Precision, recall, and F_1 are then computed on these augmented sets to quantify semantic overlap. The **Hierarchical Distance Score (HDS)** [11] compute the F_1 -score with partial credit to near-miss predictions based on the shortest-path distance between true and predicted labels in the taxonomy, penalising errors more heavily as the distance increases. Figure 2 illustrates three representative classification scenarios that highlight the complementary behaviour of taxonomy-aware metrics. In (a), a prediction that would score zero under flat F_1 receives partial credit from both hierarchical metrics due to taxonomic proximity of errors. In (b), the Overlap Score is relatively high as it rewards taxonomic consistency despite several false positives,

whereas the Distance Score penalises them more strongly. Conversely, (c) shows a case where the Distance Score remains high by rewarding semantic proximity of predictions, while the Overlap Score penalises out-of-branch errors more severely.

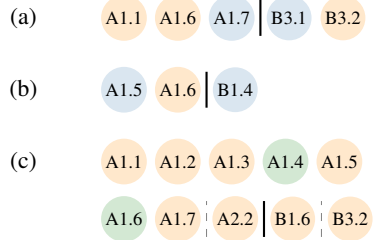


Fig. 2: Three classification examples illustrating the complementary behaviour of taxonomy-aware metrics (full taxonomy omitted). ■: true positives; ■: false positives; ■: false negatives. Vertical bars separate taxonomic branches: thick bars for main branches, thin bars for sub-branches.

2.2. Quantifying Catastrophic Abstraction Errors

We introduce the concept of a Catastrophic Abstraction Error (CAE) to capture errors that are clinically critical in hierarchical classification. For example, misclassifying a *fracture* as a *nodule* (Fig. 1) constitutes a CAE, whereas confusing it with *osteopenia* is less severe. Formally, a CAE occurs when the predicted and true label sets lie in disjoint subtrees that share only the root as a common ancestor. In Fig. 1, *nodule* belongs to the *Pulmonary and pleural diseases* branch, whereas *fracture* belongs to *Thoracic structural abnormalities*. Such errors represent a complete semantic mismatch and are not captured by flat metrics such as F_1 , which weight all false positives equally regardless of semantic distance.

2.3. Threshold Selection for Zero-Shot classification

We propose a novel *risk-constrained* threshold selection for zero-shot classification to limit the allowable CAE rate. In contrast to the normal procedure of simply maximising F_1 on the validation set (denoted *performance-based* in the paper), we add a safety constraint by selecting the threshold δ_{safety} by finding the best possible F_1 -score while making sure the CAE rate stays below a predefined maximum, τ . A key observation is that the CAE rate changes monotonically with the prediction threshold. By lowering the threshold, the model is more likely to make a correct prediction from the same branch as the ground truth, which reduces the chance of a catastrophic error. Our risk-constrained approach exploits this by choosing the threshold that achieves the best F_1 score without exceeding the pre-defined CAE limit of $\tau \leq 1\%$.

¹<https://github.com/compai-lab/2026-isbi-schaper>

²<https://huggingface.co/google/medsiglip-448>

Table 1: Multi-label classification performance of VLMs in a zero-shot setting using performance-based thresholds (Risk \times) or the proposed risk-constrained thresholds (Risk \checkmark), compared against the proposed taxonomy-aware fine-tuning. Mean and bootstrapped 95% confidence intervals are shown. All metrics are in %. Bold indicates best, underline indicates second-best.

Model	$F_1 \uparrow$	$HDS \uparrow$	$HOS \uparrow$	$CAE \downarrow$
<i>Performance-based threshold (Risk \times)</i>				
MedSigLIP	22.35 (20.23, 24.26)	21.49 (18.92, 23.90)	43.23 (41.39, 45.02)	19.5
BiomedCLIP	15.36 (13.23, 17.52)	8.71 (6.04, 11.43)	<u>40.30</u> (38.53, 42.05)	11.6
CLIP Base	11.51 (10.24, 12.83)	3.43 (1.84, 5.35)	33.27 (32.18, 34.49)	<u>0.5</u>
PubMedCLIP	9.68 (8.49, 10.82)	2.48 (0.56, 4.27)	37.64 (36.28, 38.92)	1.5
MedCLIP	14.04 (13.41, 14.69)	0.03 (0.00, 0.07)	24.52 (23.68, 25.45)	0.2
<i>Risk-constrained threshold (Risk \checkmark)</i>				
MedSigLIP	17.93 (16.69, 19.19)	8.24 (7.21, 9.58)	31.65 (30.55, 32.78)	0.9
BiomedCLIP	14.75 (13.35, 16.18)	6.98 (5.07, 9.17)	37.57 (36.09, 39.05)	2.4
CLIP Base	10.14 (9.13, 11.16)	2.32 (1.05, 3.45)	34.56 (33.34, 35.76)	1.5
PubMedCLIP	10.09 (8.78, 11.29)	3.61 (1.71, 5.37)	38.55 (37.19, 39.95)	2.2
MedCLIP	13.99 (13.33, 14.65)	0.03 (−0.03, 0.10)	24.45 (23.62, 25.36)	0.7
CLIP Base + TAF (<i>Ours</i>)	<u>21.17</u> (19.74, 22.51)	<u>15.01</u> (13.53, 16.80)	33.69 (32.56, 34.81)	1.6

2.4. Taxonomy-Aware Fine-Tuning

To reduce severe CAEs, we evaluate two complementary fine-tuning strategies, each designed to improve alignment with the PadChest-GR taxonomy. First, **SigLIP Fine-Tuning**, an in-domain adaptation without hierarchy, fine-tune a general-domain model using SigLIP’s pairwise sigmoid loss [12] on the PadChest-GR [4], which includes finding sentences and labels. Freeze the vision and text encoders, updating only the projection layers to control efficiency and prevent overfitting, testing whether in-domain adaptation alone can reduce catastrophic errors. Secondly, **Radial Embedding (RE) Fine-Tuning** [13], an explicit hierarchical encoding strategy, leverages an RE loss to adjust the concept embeddings’ radial distances from the hierarchy’s root, explicitly separating incompatible branches. Root and branches are defined by adapting the HierarCaps framework [13] to PadChest-GR by constructing, for each finding, a “positive chain” following its root-to-leaf path and a “negative chain” by substituting a mutually exclusive sibling. For instance, the finding “*Signs of air trapping*” is linked to the following positive chain: “*Pulmonary and Pleural Diseases*” (abstract) \rightarrow “*Pulmonary Patterns*” \rightarrow “*Hyperinflated lung*” \rightarrow “*Signs of air trapping* (specific)”. Negative chains are created by substituting mutually exclusive siblings at each level of abstraction, e.g., substituting “*Pulmonary and Pleural Diseases*” with “*Thoracic Structural Abnormalities*”. We freeze the vision encoder to preserve the original multimodal alignment.

3. EXPERIMENTS AND RESULTS

3.1. Taxonomy-Aware Fine-Tuning

Table 1 reports the zero-shot multi-label classification results. In the standard setting (top table), MedSigLIP achieves the highest performance across F_1 , HDS, and HOS metrics, followed by BiomedCLIP. However, both models exhibit CAE rates above 10%, indicating misalignment with medical taxonomies despite their strong overall performance. Mod-

els with lower CAE rates achieve much lower F_1 scores, highlighting a trade-off between predictive accuracy and catastrophic error reduction. To address the misalignment observed in the zero-shot setting, we apply the proposed *risk-constrained threshold* (bottom table), which directly targets catastrophic errors by adjusting the decision threshold to keep CAE rates below a predefined limit. This reduces CAE to below 2.4%, effectively eliminating most cross-branch misclassifications highlighted earlier. While this comes at the cost of a moderate drop in F_1 , the improvement in semantic consistency demonstrates that threshold optimisation is an effective first step toward aligning VLM predictions with medical taxonomies. However, it cannot recover the performance lost. To address this, we proposed a *taxonomy-aware fine-tuning* strategy, which explicitly aligns the embedding space with the hierarchical structure of medical findings (CLIP Base + TAF). As shown in Table 1, our approach achieves competitive F_1 performance compared to MedSigLIP in the performance-based setting, while keeping CAE rates low — a combination that neither zero-shot models nor risk-constrained thresholding alone can offer. The ablation study in Table 2 further highlights the complementary roles of each component. We find that *performance-based* thresholding yields the highest F_1 but allows many catastrophic errors to persist, even with fine-tuning. Under the *risk-constrained* threshold, CAE rates are successfully controlled, and the combination of SigLIP fine-tuning with radial embedding yields the best balance, maximising performance while minimising severe cross-branch errors. Also, radial embedding fine-tuning alone does not provide improvement over the baseline, indicating that hierarchical supervision without domain adaptation (SigLIP fine-tuning) is insufficient in this setting.

3.2. Representation Alignment with Taxonomy

Finally, we analyse whether the improved performance corresponds to better alignment between the model’s representation space and the medical taxonomy. Using Kendall’s τ

Table 2: Ablation Study of the Fine-Tuning strategy using performance-based (Perf.) or risk-constrained (Risk) threshold. RE: Radial Embedding. Bold indicates best, underline indicates second-best. ■ highlights CAE-critical values; ■ indicates best results with CAE below 5%.

	SigLIP	RE	$F_1 \uparrow$	HDS \uparrow	HOS \uparrow	CAE \downarrow
Perf.			11.51	3.43	33.27	0.50
	✓	✓	10.80	1.19	30.73	<u>1.10</u>
	✓	✓	24.38	19.60	39.02	35.60
Risk			21.79	<u>17.99</u>	<u>37.30</u>	6.40
		✓	10.14	2.32	34.56	1.50
	✓	✓	10.87	1.37	31.06	1.80
			17.33	5.71	30.26	3.50
		✓	21.17	15.01	33.69	1.60

Table 3: Kendall’s τ rank correlation between model predictions and PadChest-GR taxonomy ordering on the test set. Mean \pm SD across all root-to-leaf paths. Higher indicates stronger preservation of taxonomic abstraction order.

Model	Ours	PubMedCLIP	CLIP Base	MedCLIP	MedSigLIP	BiomedCLIP
Kendall’s τ	0.86 \pm	<u>0.72 \pm</u>	0.25 \pm	0.19 \pm	-0.17 \pm	-0.69 \pm
SD	0.27	0.38	0.48	0.43	0.55	0.51

rank correlation [13], which measures whether model representations preserve the semantic ordering from general to specific concepts, we find that our hierarchically fine-tuned model achieves $\tau = 0.86$, a substantial improvement over the CLIP Base baseline ($\tau = 0.25$), confirming that radial embedding fine-tuning effectively encodes hierarchical relationships. In contrast, several medical-domain VLMs exhibit poor or even negative alignment, with BiomedCLIP showing strong anti-correlation ($\tau \approx -0.69$). These results suggest that improved taxonomy alignment translates into lower CAE rates, linking the quantitative performance gains to meaningful changes in representation geometry.

4. CONCLUSION

This work investigated how to quantify and mitigate abstraction errors of VLMs in multi-label CXR classification using hierarchical metrics and taxonomy-aware methods. We first showed that SOTA VLMs remain misaligned with medical taxonomies under hierarchical evaluation, with standard flat metrics obscuring severe cross-branch errors. To capture these clinically critical mistakes, we introduced Catastrophic Abstraction Errors (CAEs), a hierarchical metric tailored to the multi-label setting. Finally, we proposed lightweight mitigation strategies, including risk-constrained thresholding for zero-shot classification and taxonomy-aware fine-tuning with radial embeddings, which substantially reduce severe abstraction errors without compromising overall performance. Our results show that hierarchical evaluation, risk-aware inference, and representation-level alignment provide a path toward safer and more clinically reliable multimodal models.

5. REFERENCES

- [1] A. Radford *et al.*, “Learning Transferable Visual Models From Natural Language Supervision,” in *International Conference on Machine Learning*, 2021, pp. 8748–8763.
- [2] Y. Zhang *et al.*, “Contrastive learning of medical visual representations from paired images and text,” vol. 182, 2022, pp. 2–25.
- [3] A. E. W. Johnson *et al.*, “Mimic-cxr-jpg, a large publicly available database of labeled chest radiographs,” 2019. [Online]. Available: <https://arxiv.org/abs/1901.07042>
- [4] D. C. Castro *et al.*, “Padchest-gr: A bilingual chest x-ray dataset for grounded radiology report generation,” 2024. [Online]. Available: <https://arxiv.org/abs/2411.05085>
- [5] Z. Wang *et al.*, “MedCLIP: Contrastive Learning from Unpaired Medical Images and Text,” *ACL Anthology*, pp. 3876–3887, 2022.
- [6] S. Eslami, C. Meinel, and G. de Melo, “PubMedCLIP: How much does CLIP benefit visual question answering in the medical domain?” in *Findings of the Association for Computational Linguistics: EACL 2023*, 2023, pp. 1181–1193.
- [7] S. Zhang *et al.*, “A Multimodal Biomedical Foundation Model Trained from Fifteen Million Image–Text Pairs,” *NEJM AI*, 2024.
- [8] J. Hirsch *et al.*, “Icd-10: History and context,” *American Journal of Neuroradiology*, vol. 37, no. 4, pp. 596–599, 2016.
- [9] K. C. Wang, “Standard lexicons, coding systems and ontologies for interoperability and semantic computation in imaging,” *Journal of Digital Imaging*, vol. 31, no. 3, pp. 353–360, 2018.
- [10] S. Kiritchenko and F. Famili, “Functional annotation of genes using hierarchical text categorization,” *Proceedings of BioLink SIG, ISMB*, 2005.
- [11] A. Kosmopoulos *et al.*, “Evaluation measures for hierarchical classification: a unified view and novel approaches,” *Data Mining and Knowledge Discovery*, vol. 29, no. 3, pp. 820–865, 2014.
- [12] X. Zhai *et al.*, “Sigmoid loss for language image pre-training,” in *Proceedings of the IEEE/CVF International Conference on Computer Vision (ICCV)*, 2023, pp. 11975–11986.
- [13] M. Alper and H. Averbuch-Elor, “Emergent visual-semantic hierarchies in image-text representations,” in *Proceedings of the European Conference on Computer Vision (ECCV)*, 2024.